Simulation and Optimization of Supercritical Fluid Purification of Phytosterol Esters

Tiziana Fornari, Carlos F. Torres, F. Javier Señoráns, and Guillermo Reglero
Sección Departamental de Ciencias de la Alimentación, Universidad Autónoma de Madrid, 28049 Cantoblanco, Madrid, Spain

DOI 10.1002/aic.11728
Published online February 19, 2009 in Wiley InterScience (www.interscience.wiley.com).

Supercritical carbon dioxide extraction to separate phytosterol esters from fatty acid esters and tocopherols was simulated and optimized using the group contribution equation of state. Experimental extraction data at 328 K, pressures ranging from 200 to 280 bar and solvent-to-feed ratio around 25, was employed to verify the performance of the thermodynamic model. The raw material is the product obtained after a two-step enzymatic reaction carried out on soybean oil deodorizer distillates, and contains mainly fatty-acid ethyl esters, tocopherols and phytosterol esters. The extraction process was simulated using model substances to represent the complex multicomponent feed material. Nonlinear programming techniques were applied to find out optimal process conditions for a steady-state countercurrent process with partial reflux of the extract. The process optimization procedure predicts that a product with 94.2 wt % of phytosterol ester purity and 80% yield could be achieved. © 2009 American Institute of Chemical Engineers *AIChE J,* 55: 1023–1029, 2009

Keywords: phytosterol esters, countercurrent extraction, phase equilibria, supercritical process, group contribution

Introduction

Plant sterols, stanols and their esters have received increasing attention during the last decade because of their beneficial physiological functions in humans.[1–4] In general, esterified sterols and stanols are preferred than their free forms.[5] The practical applications of free phytosterols in foods are limited by their low solubility in lipid-type foods, their crystalline structure and their easy reactivity. For example, the solubility of phytosterols in edible oils is very low (2–3%), while their melting points are rather high (413–423 K).[4] Esterification of phytosterols can be used to produce a more soluble product, which can be incorporated in fat-based products, but maintaining phytosterol bioefficiency.

In previous work,[6] soybean oil deodorizer distillate (SODD) was enzymatically modified to obtain a product mixture containing mainly phytosterol esters, tocopherols, and fatty acid ethyl esters. Then, carbon dioxide supercritical fluid extraction (CO_2-SFE) of this mixture was employed in order to produce a raffinate product comprised mainly of phytosterol esters.[7] SFE demonstrated to be an efficient fractionation process, since a raffinate product with 82.4 wt % of phytosterol esters at 250 bar, 328 K and solvent-to-feed ratio of 35 was obtained in a one-meter packed column (without reflux).

This work presents the thermodynamic modeling of the countercurrent CO_2-SFE process of a raw material comprising phytosterol esters, tocopherols and fatty acid ethyl esters (the enzymatic modified SODD). The analysis carried out in our laboratory provided the following composition (weight basis): fatty-acid ethyl esters (FAEE) 30.0%, tocopherols (TOC) 17.5%, phytosterol esters (PE) 38.6% and minor amounts of triacylglycerides (4.2%), squalene (3.3%), free fatty-acids (4.1%) and free sterols (2.3%).

The thermodynamic model applied is the GC-EoS.[8,9] This model has been already used by several authors in the simu-

Correspondence concerning this article should be addressed to T. Fornari at tiziana.fornari@uam.es.

Table 1. Representation of the Real Multicomponent Feed Material by Model Substances in the GC-EoS Thermodynamic Modeling

Real Feed Mixture[a]		% wt	Model Feed Mixture	% wt (normalized)
Light fraction	Squalene	3.3	Ethyloleate	34.1
	Fatty acid ethyl esters	30.0		
Light key component	Free fatty acids	4.1	α-Tocopherol	22.1
	Tocopherols	17.5		
Heavy key component	Phytosterol esters	38.6	Sitosteryl oleate	39.5
Heavy fraction	Triacylglycerides	4.2	Triolein	4.3

[a]Also contains 2.2%wt of free sterols which were not considered in the thermodynamic modeling.

lation and optimization of different supercritical processes related with lipid-type materials, such as the fractionation of fatty-acid esters,[10] the deterpenation of citrus essential oils,[11] the concentration of squalene from olive oil sources,[12] the supercritical hydrogenation of oils,[13] etc. In this work, the GC-EoS was used to represent the phase equilibrium behavior of the multicomponent raw material (represented via a careful selection of model substances), and the supercritical CO_2 solvent. The simulation of the extraction processes was supported by an accurate representation of the vapor-liquid equilibria of the CO_2 + model substance binary mixtures. Experimental SFE yields and compositions[7] were satisfactorly calculated using the GC-EoS, and, thus, the model was employed to optimize the extraction process in terms of phytosterol ester yield and purity.

The GC-EoS model

The GC-EoS[8,9] is an equation of state originally developed for both nonpolar and polar components. The residual Helmholtz energy of the system is calculated assuming two contributions: a free volume repulsive term, and a contribution which accounts for energy attractions among groups.

The GC-EoS repulsive term is modeled assuming hard-sphere behavior for the molecules and each substance is characterized by its critical hard-sphere diameter d_{ci}. In the original model,[8] the d_{ci} values are calculated from critical properties for gases, and for solvents are fitted to pure component vapor pressure data. The GC-EoS attractive term is a group-contribution version of the NRTL model, and has five pure-group parameters (T^*, q, g^*, g' and g'') and four binary interaction parameters (K_{ij}^*, K_{ij}', α_{ij} and α_{ji}). A detail description of the model equations is given in the Appendix, together with the values of the parameters employed in this work.

Results and discussion

SFE Process Simulation. The SFE process was mathematically solved within a sequential process simulator that includes rigorous models for a high-pressure multistage extractor[15] and a multiphase flash.[16] In these routines (FORTRAN language) thermodynamic phase equilibria calculations were performed using the GC-EOS model.

The fatty-acid profile of the enzymatic modified SODD indicates that the raw material contains around 45 wt % of oleic acid. Thus, ethyloleate and triolein were selected to represent, respectively, the lightest and heaviest fractions. Additionally, α-tocopherol was selected to represent all tocopherol isomers detected by the chemical analysis. For these model substances selected, that is, ethyloleate, triolein and α-tocopherol, abundant binary phase equilibria data with supercritical CO_2 is available in the literature.[17–21]

The PE fraction was represented using sitosteryl oleate as model substance since sitosterol is the main free sterol present in soybean oil, and oleic acid was the free fatty-acid employed in the esterification enzymatic reaction. In this case, no binary CO_2 + steryl ester vapor-liquid equilibria data was found in the literature.

Table 1 compares the composition of the real multicomponent feed mixture (as obtained by the chemical analysis), and the model feed mixture employed in the simulation procedure. Based on the volatility and solubility of the substances, and by analogy with a traditional distillation process, the key light and heavy components are, respectively, α-tocopherol and sitosteryl ester.

Previous works have demonstrated the capability of the GC-EoS model to represent high-pressure phase equilibria in mixtures containing CO_2 and lipid-type products such as triacylglycerides,[22] tocopherols,[23] fatty acid alkyl esters,[10] and squalene,[12] and so on. Providing the adequate parameter table a large number of substances can be represented by using the group contribution approach. As an example, Figure 1 shows a comparison between experimental and calculated equilibrium constants (k_i = weight fraction in vapor phase/weight fraction in liquid phase) of ethyloleate, oleic acid, squalene, α-tocopherol and triolein in binary mixtures with CO_2. The corresponding pure group and binary interaction parameters (employed in the phase equilibria representation depicted in Figure 1) were obtained from the recent revision of the GC-EoS parameter table presented by Fornari,[24] and are reproduced in the Appendix. With respect to the k_i values depicted in Figure 1, average absolute relative deviations (*AARD*)

$$AARD = \frac{1}{N_{\text{exp}}} \sum \left| \frac{k_i^{\text{exp}} - k_i^{\text{cal}}}{k_i^{\text{exp}}} \right| \tag{1}$$

were, respectively, 8.6% for ethyloleate, 15.7% for oleic acid, 19.4% for squalene, 12.8% for α-tocopherol, and 26.2% for triolein.

The pure component parameters required by the GC-EoS model in the phase equilibria calculations are given in Table 2. Critical temperatures were calculated using Fedors[25] or Joback et al.[26] (if the normal boiling point of the pure compound is known) group contribution methods. Critical hard-sphere molecular diameters (d_c) were optimized to the corresponding binary CO_2 + model substance vapor-liquid

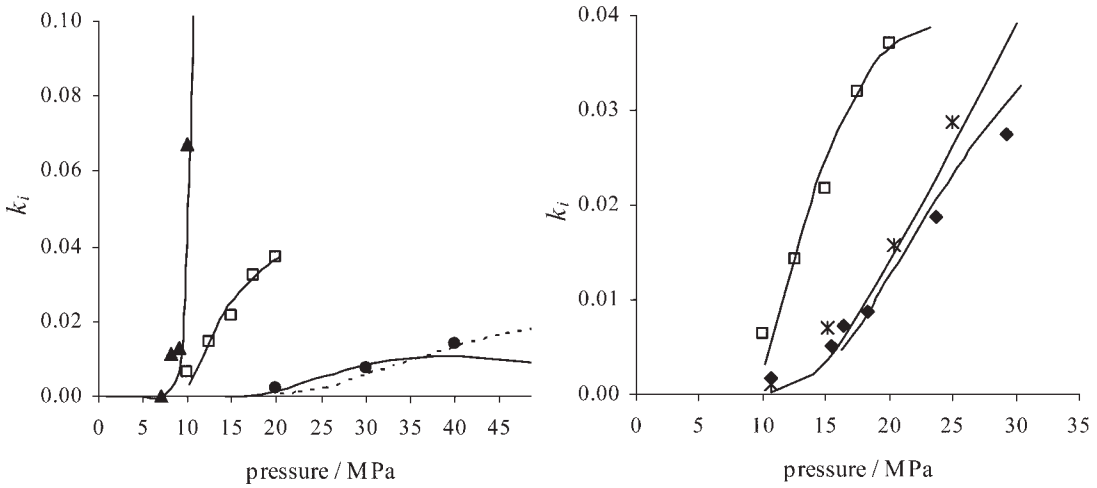

Figure 1. Experimental (symbols) and GC-EoS (solid lines) equilibrium constants (k_i = weight fraction in vapor phase/weight fraction in liquid phase) of triolein (●) at 333 K[20]; ethyloleate (▲) at 313 K[17]; oleic acid (*) at 333 K[30]; α-tocopherol (◆) at 333 K[19], and squalene (□) at 313 K[31] in mixture with CO_2 Dotted lines: GC-EoS calculations for $d_{c\ \text{triolein}} = 11.535$ and $K^*_{\text{TG-CO2}} = 1.190$.

equilibrium data in order to improve the original GC-EoS prediction. Table 2 shows that the d_c values resulted for ethyloleate and α-tocopherol are reasonably similar to the values obtained from pure component vapor pressure data. For triolein, the optimal d_c value obtained ($d_{c\ \text{triolein}} = 11.535$) is somewhat different from the value regressed from infinite dilution activity coefficient data.[14] This is for the reason that the interaction parameter $K^*_{\text{TG-CO2}}$ (i.e., between the triglyceride group and CO_2) was also re-adjusted. The $K^*_{\text{TG-CO2}}$ value obtained (1.190) is comparable to the original value[24] (1.094), but considerably improves the triolein equilibrium constants (see Figure 1) particularly at very high-pressures (*AARD* was reduced from 26.2% to 15.7%).

The estimation of sitosteryl oleate d_c value was difficult to carry out due to the lack of pure component vapor pressure data or CO_2 + steryl ester vapor-liquid equilibrium data. The dependence of the d_c parameter of homologous series of compounds (alkanes, alkenes, triacylglycerols, fatty-acid alkyl esters, fatty-acids, etc.) with molecular weight,[24] carbon number[27] or van der Waals volume,[14] was previously demonstrated in the literature. On the basis of these approaches, the sitosteryl oleate d_c value was obtained from the correlation of the d_c values of high-molecular-weight compounds with their corresponding molecular weights as shown in Figure 2. Although the compounds employed to develop the correlation do not belong to a homologous series, all of them contains a large number of paraffin groups in their chemical structure.

Table 2. Pure Component Parameters Used in the GC-EoS Thermodynamic Modeling

Component	Molecular Weight	T_c (K)	d_c (cm/mol) This Work	d_c (cm/mol) Previous Works
Ethyloleate	310	784.2	8.151	8.078[b]
α-Tocopherol	431	857.4	9.015	8.858[c]
Sitosteryl oleate	679	950.1	10.622[a]	
Triolein	884	1020	11.535	11.839[d]

[a]Calculated according the correlation presented in Figure 2.
[b]Estimated from normal boiling point.
[c]Estimated from boiling point at 0.0688 bar.
[d]Estimated from infinite dilution activity coefficients.[14]

The flow sheet of the simulated SFE extraction process is shown in Figure 3. No partial reflux of the extract was considered since the experimental extractions were carried out without reflux. Additionally, three stages were the number of theoretical stages that better fitted all experimental countercurrent extraction data. A comparison between the experimental and calculated raffinate compositions and PE yield (amount of PE in raffinate/amount of PE in feed) is given in Table 3, and depicted in Figure 4 as a function of pressure

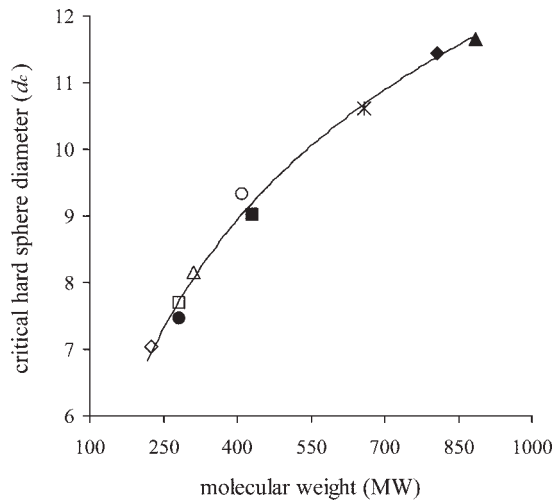

Figure 2. Correlation of the d_c (cm/mol) values of high-molecular-weight (MW) compounds: $d_c = 3.486 \times \ln(\text{MW}) - 12.105$ ($R^2 = 0.99$). (◇) hexadecane; (●) oleic acid; (□) eicosane; (△) ethyloleate; (○) squalene; (■) α-tocopherol; (◆) tripalmitin; (▲) triolein. Sitosteryl oleate d_c value (*) was calculated according to the correlation.

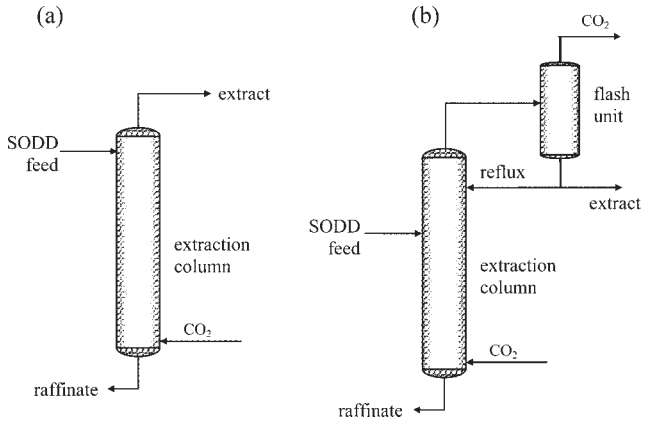

Figure 3. Flow sheet of the SFE process simulated (a), and optimized (b).

(experiments 1 to 4). FAEE were almost completely eliminated (FAEE yields in top product higher than 97%) in all experimental SFE assays reported in Table 3. Thus, as mentioned before, the separation problem studied is the partition of phytosterol esters and tocopherols between the top product and bottom product; to concentrate phytosterol esters in the raffinate is necessary the extraction of tocopherols but maintaining a high phytosterol ester yield.

The experimental composition range (i.e., the difference between the maximum and minimum composition measured) for FAEE, TOC, PE and TAG was, respectively, 0.8, 17.4, 17.2 and 1.4 (see Table 3), while the average absolute difference between experimental and calculated values was, correspondingly, 0.1, 2.6, 2.6 and 1.1. Thus, deviations between experimental and calculated FAEE and TAG compositions may not be significant. For example, it can be recognized that almost no FAEE was present in all experimental raffinates, and that the GC-EoS model predicts the same behavior, but no statistical error between experimental and calculated FAEE composition values can be accurately established. Thus, only average absolute relative deviations (*AARD*) related with PE and TOC compositions were considered to evaluate the model performance.

Good agreement was achieved between experimental and calculated values. *AARD* were, respectively, 4.4% and 15.6% for PE and tocopherol composition (wt %) in the raffinate, and *AARD* was 7.3% in the calculation of PE yield.

Additionally, inspection of Table 3 show that the model can adequately predict the effect of the solvent-to-feed (S/F) ratio on the raffinate composition and PE yield. As expected, experiments 1 and 5 show that lower S/F ratios produced an increase in PE yield, but a decrease in PE purity (from 69.2 to 65.2%). Further, an increase of the S/F ratio from 25 to 35 (experiments 3 and 6) resulted in the opposite effect. The GC-EoS can reasonably follow these variations, although the effect on PE yield is somewhat overestimated.

With respect to the temperature effect on the SFE process, it has to be pointed out that only two extraction temperatures were explored at 225 bar and S/F = 25. A comparison between experiments 2 and 7 indicates that a change in the extraction temperature from 328 to 318 K has almost no effect on the raffinate. On the other side, the GC-EoS model predicts that the selectivity of the process toward the extraction of tocopherols was increased, because PE composition was considerably increased from 69.9 to 78.1%. This discrepancy with respect to temperature variations should be further investigated in order to validate the results obtained in the following section.

SFE Process Optimization. The SFE process simulation model was used to optimize process conditions in order to improve phytosterol ester yield and purity. The extraction scheme comprises the countercurrent extraction column and one separator (flash) unit. The liquid phase from the flash tank is partly returned to the extractor column as reflux, and partly recovered as the extract product (Figure 3b). The vapor phase is the recovered CO_2 solvent, which can be recycled to the extraction column.

The optimization procedure utilized a nonlinear programming model that includes continuous optimization variables (x), and integer variables (y)

$$\mathrm{Max}_{x,y} f(x,y)$$
$$s.t.$$
$$h(x,y) = 0$$
$$g(x,y) < 0$$

Table 3. Composition and Yield Obtained in Raffinate Product of the CC-SFE Assays Carried Out at the Different Extraction Conditions: Comparison Between Experimental[7] Results and Values Calculated by Using The GC-EoS Model

					Raffinate Composition (%wt Solvent Free Basis)				
	P (bar)	S/F	T (K)		FAEE (+ squalene)	TOC (+ free fatty acids)	PE	TAG	PE yield (%)
1	200	25	328	exp	0.5	23.5	69.2	6.8	74.1
				cal	0.3	25.8	65.9	7.9	82.0
2	225	25	328	exp	0.1	17.4	74.8	7.7	69.9
				cal	0.2	21.4	69.9	8.5	71.9
3	250	25	328	exp	0.1	14.7	77.9	7.3	61.5
				cal	0.1	15.7	75.3	8.9	65.5
4	280	25	328	exp	0.1	12.2	79.7	8.0	58.1
				cal	0.1	9.4	82.0	8.5	56.4
5	200	15	328	exp	0.9	27.3	65.2	6.6	75.7
				cal	1.2	29.8	62.6	7.2	88.7
6	250	35	328	exp	0.1	9.9	82.4	7.6	57.9
				cal	0.0	7.7	82.2	10.1	50.8
7	225	25	318	exp	0.1	16.6	75.9	7.4	70.8
				cal	0.1	13.5	78.1	8.3	74.8

FAEE: fatty acid ethyl ester, TOC: tocopherols, PE: phytosterol esters, TAG: Triacylglycerides.

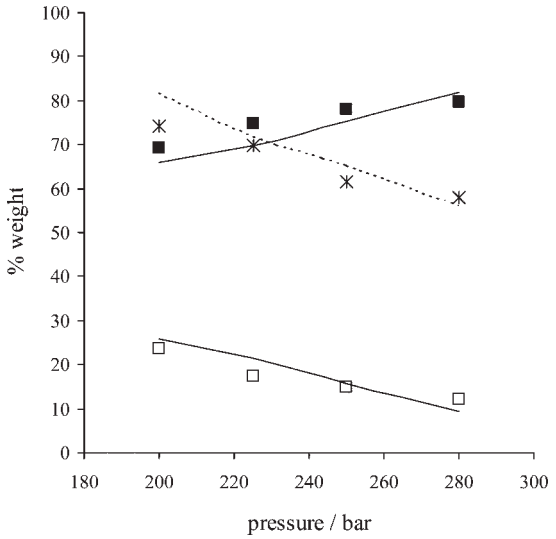

Figure 4. Comparison between experimental[7] and calculated raffinate composition and PE yield obtained at 328 K, S/F = 25 and different extraction pressures: (■) experimental PE and (□) TOC composition; (*) experimental PE yield; (——) calculated PE and TOC compositions, and (– – –) calculated PE yield.

Equality constraints (h) represent the mathematical simulation model of the SFE process; inequality constraints (g) include process specifications and operating bounds and $f(x,y)$ is the objective function. The optimization is performed integrating the rigorous sequential modular simulator with the optimization program.[28] The optimization algorithm is an *ad hoc* extension of the outer approximations[29] that interacts with the process simulator in a black box way.

The number of theoretical stages and feed stage were the integer variables. In order to explore the variation of PE purity, and yield with these variables different simulations were carried out at 280 bar, 328 K, S/F = 25 and considering a reflux stream introduced from the top. The reflux ratio, defined as

$$\text{reflux ratio} = \frac{\text{reflux mass flow}}{\text{reflux mass flow} + \text{extract mass flow}}$$

was set to 0.5, denoting that the liquid stream of the flash unit is divided in two equal mass-flow streams (the reflux and the extract streams). Table 4 shows that eight theoretical stages, being the fourth (from top) the feed stage, is an adequate separation scheme. Therefore, these integer variables have been fixed and only continuous variables were considered in the optimization procedure. This reduces the mathematical complexity of the problem (i.e., only continuous variables were optimized) without considerable loss of accuracy.

The objective function was to maximize PE concentration in the raffinate product. The continuous optimization variables were: extraction pressure and temperature, solvent flow rate and reflux ratio. The pressure and temperature of the flash unit were set to 60 bar and 328 K, since slight effect of these variables on the objective function were detected when varied in the usual ranges (40–60 bar and 313–333 K). Inequality constraints include PE recovery (≥80%), CO_2 purity (≥99.9 wt %) and operating bounds as described in Table 5. The extraction pressure and temperature bounds were setup in the range were the phase equilibria of binary CO_2 + model substance was proved to be satisfactory correlated by the GC-EoS model.

The optimal process variables obtained are shown in Table 5, and resulted in a raffinate product with 94.2 wt % of PE (5.3 wt % triglycerides and 0.5 wt % tocopherols) and 80% PE recovery.

Taking into consideration that PE are more readily extracted than TAG (as suggested in Table 1), the maximum PE purity in the raffinate could be 90.2 wt %. Nevertheless, the optimal solution attained by the optimization procedure resulted in PE purity greater than this value. This is explained by a change in the relative volatility between PE and TAG (k_{PE}/k_{TAG}) from values greater than unity to values lower than unity, predicted by the GC-EoS model while increasing pressure. Yet, it has to be point out that although the model is based on an accurate phase equilibria representation of the binaries CO_2 + ethyloleate, CO_2 + tocopherol and CO_2 + triolein, no guarantee about the CO_2 + sitosteryl oleate phase equilibria calculation can be established due to the lack of experimental data found in the literature.

Table 4. Variation of Phytosterol Ester (PE) Purity and Yield with the Number of Theoretical Stages and Feed Stage at 280 bar, 328 K and S/F = 25

Number of Theoretical Stages	Feed Stage	% wt PE in Raffinate	PE Yield (%)
reflux ratio = 0.0			
3	1	82.0	56.4
reflux ratio = 0.5			
3	2	73.3	82.5
4	2	75.5	83.6
6	2	76.6	84.3
8	2	76.7	84.4
10	2	76.8	84.4
12	2	76.8	84.4
reflux ratio = 0.5			
8	2	76.7	84.4
8	3	78.4	85.7
8	4	79.2	86.4
8	5	79.3	86.5

Table 5. Inequality Constrains, Lower and Upper Bounds Employed and Optimal Values Obtained in the Optimization of the CC-SFE Process

Variable	Lower Bound	Upper Bound	Optimal Value
Extraction pressure (bar)	200	300	300
Extraction temperature (K)	313	343	324
Solvent to feed ratio (kg/kg)	20	50	42.7
Reflux ratio	0.5	1.5	0.48
PE yield in raffinate	≥80		80.
PE concentration %wt (objective function)			94.2

Conclusions

Thermodynamic simulation and optimization of the purification of phytosterol esters from an enzymatic modified SODD using supercritical CO_2 was studied in this work. The composition of the raw material set out the separation of phytosterol esters from tocopherols and fatty-acid alkyl esters. Previous experimental SFE demonstrate that a countercurrent packed column of 1 m height can increase phytosterol concentration from 38 wt % to c.a. 80 wt % working at high-extraction pressures (250–280 bar).

The GC-EoS model was applied to simulate the countercurrent SFE process. The group interaction parameters and the pure substance parameters employed were from the literature or adjusted to binary vapor-liquid data. Thus, the GC-EoS model was applied in a completely predictive manner to simulate the phase equilibria behavior of CO_2 and the complex multicomponent mixture in a multistage separation process. The great advantage of the group contribution approach, and the appropriate selection of model substances to represent the complex multicomponent feed allowed a fast, simple and satisfactory simulation of the SFE process.

Nonlinear optimization techniques were used to improve PE concentration in the raffinate product, maintaining a high PE recovery. The computer aided optimization of the extraction process, including partial reflux of the extract, result in a raffinate product with 94.2 wt % phytosterol ester purity and 80% recovery. An experimental study, using an extraction column with partial reflux of the extract, has to be carried out in order to confirm the computer-aided optimal solution predicted by the model.

Acknowledgments

The authors gratefully acknowledge the financial support from the Comunidad Autónoma de Madrid (ALIBIRD, project S-505/AGR-0153) and the Ministerio de Ciencia y Tecnología, projects AGL2008-05655/ALI and 25506 FUN-C-FOOD (CONSOLIDER-INGENIO 2010), Spain. T. Fornari and C. Torres would like to acknowledge the postdoctoral contract (Programa Ramón y Cajal), given by the Ministerio de Ciencia y Tecnología and the Universidad Autónoma de Madrid, Spain.

Literature Cited

1. Jones PJH, Ntanios FY, Raeini-Sarjaz M, Vanstone CA. Cholesterol-lowering efficacy of a sitostanol-containing phytosterol mixture with a prudent diet in hyperlipidemic men. *Am J Clin Nutr*. 1999;69: 1144–1150.
2. Sierksma A, Weststrate JA, Meijer GW. Spreads enriched with plant sterols, either esterified 4,4-dimethylsterols or free 4-desmethylsterols, and plasma total- and LDL-cholesterol concentrations. *Br J Nutr*. 1999;82:273–282.
3. Quilez J, García-Lorda P, Salas-Salvado J. Potential uses and benefits of phytosterols in diet: present situation and future directions. *Clin Nutr*. 2003;22:343–351.
4. Wester I. Cholesterol-lowering effect of plant sterols. *Eur J Lipid Sci Tech*. 2000;102:37–44.
5. Nestel P, Cehun M, Pomeroy S, Abbey M, Weldon G. Cholesterol lowering effects of plant sterol esters and non-esterified stanols in margarine, butter and low-fat foods. *Eur J Clin Nutr*. 2001;55:1084–1090.
6. Torres CF, Torrelo G, Señorans FJ, Reglero G. A two steps enzymatic procedure to obtain sterol esters, tocopherols and fatty acid ethyl esters from soybean oil deodorizer distillate. *Proc Biochem*. 2007;42:1335–1341.
7. Torres CF, Fornari T, Torrelo G, Señoráns FJ, Reglero G. Production of phytosterol esters from soybean oil deodorizer distillates. accepted in *Eur J Lipid Sci Tech*. Dec. 2008.
8. Skjold-Jørgensen S. Gas solubility calculations II. Application of a new group-contribution equation of state. *Fluid Phase Equilib*. 1984;16:317–351.
9. Skjold-Jørgensen S. Group contribution equation of state (GC-EOS): A predictive method for phase equilibrium computations over wide ranges of temperatures and pressures up to 30 MPa. *Ind Eng Chem Res*. 1988;27:110–118.
10. Espinosa S, Diaz S, Brignole EA. Thermodynamic modeling and process optimization of supercritical fluid fractionation of fish oil fatty acid ethyl esters. *Ind Eng Chem Res*. 2002;41:1516–1527.
11. Diaz S, Espinosa S, Brignole EA. Citrus peel oil deterpenation with supercritical fluids optimal process and solvent cycle design. *J Supercrit Fluids*. 2005;35:49–61.
12. Vázquez L, Torres CF, Fornari T, Señoráns FJ, Reglero G. Recovery of squalene from vegetable oil Sources using countercurrent supercritical carbon dioxide extraction. *J Supercrit Fluids*. 2007;40:59–66.
13. Pereda S, Bottini SB, Brignole EA. Gas-liquid reactions under supercritical conditions - phase equilibria and thermodynamic modeling. *Fluid Phase Equilib*. 2002;194–197:493–499.
14. Espinosa S, Fornari T, Bottini SB, Brignole EA. Phase equilibria in mixtures of fatty oils and derivatives with near critical fluids using the GC-EoS. *J Supercrit Fluids*. 2002;23:91–102.
15. Brignole EA, Andersen PM, Fredenslund AA. Supercritical fluid extraction of alcohols from water. *Ind Eng Chem Res*. 1987;26:254–261.
16. Michelsen ML. The isothermal flash problem. Part II. Phase-split calculation. *Fluid Phase Equilibr*. 1982;9:21–40.
17. Bharath R, Inomata H, Arai K, Shoji K, Noguchi Y. Vapor-liquid equilibria for binary mixtures of carbon dioxide and fatty acid ethyl esters. *Fluid Phase Equilib*. 1989;50:318–327.
18. Pereira PJ, Gonçalvez M, Coto B, Gomes de Azevedo E, Nunes da Ponte M. Phase equilibria of CO_2^+ dl-α-tocopherol at temperatures from 292 K to 333 K and pressures up to 26 MPa. *Fluid Phase Equilib*. 1993;91:133–143.
19. Fang T, Goto M, Yun Z, Ding X, Hirose T. Phase equilibria for binary systems of methyl oleate-supercritical CO2 and a-tocopherol-supercritical CO_2. *J Supercrit Fluids*. 2004;30:1–16.
20. Weber W, Petkov S, Brunner G. Vapour-liquid-equilibria and calculations using the Redlich-Kwong-Aspen-equation of state for tristerarin, tripalmitin and triolein in CO_2 and propane. *Fluid Phase Equilib*. 1999;158–160:695–706.
21. Bharath R, Inomata H, Adschiri T, Arai K. Phase equilibria study for the separation and fractionation of fatty oil components using supercritical carbon dioxide. *Fluid Phase Equilib*. 1992;81:307–320.
22. Florusse LJ, Van't Hof A, Fornari T, Bottini SB, Peters CJ. Phase behavior of binary systems of carbon dioxide and certain low-molecular weight triglycerides: measurements and thermodynamic modeling. *J Supercrit Fluids*. 2004;31:123–132.
23. Espinosa S, Díaz S, Fornari T. Extension of the group contribution associating equation of state to mixtures containing phenol, aromatic acid and aromatic ether compounds. *Fluid Phase Equilib*. 2005;231:197–210.
24. Fornari T. Revision and summary of the group contribution equation of state parameter table: application to edible oil constituents. *Fluid Phase Equilib*. 2007;262:187–209.
25. Reid R, Prausnitz JM, Poling B. *The Properties of Gases and Liquids*. 4th ed. New York: Mc Graw-Hill Book Company; 1987.
26. Joback KG, Reid RC. Estimation of pure-component properties from group contributions. *Chem Eng Commun*. 1983;57:233–239.
27. Fornari T, Bottini SB, Brignole EA. Application of a group contribution equation of state to mixtures of supercritical gases with natural fatty oils and derivatives. *Lat Am Appl Res*. 2001;31:287–291.
28. Diaz S, Serrani A, de Beistegui R, Brignole EA. A MINLP strategy for the debottlenecking problem in an ethane extraction plant. *Comp Chem Eng*. 1995;19:175–180.
29. Duran M, Grossmann IE. A mixed-integer nonlinear programming approach for process systems synthesis. *AIChE J*. 1986;32:592.
30. Zer-Ran Y., Rizvi SSH, Zollweg JA. Phase equilibria of oleic acid, methyl oleate and anhydrous milk fat in supercritical carbon dioxide. *J Supercrit Fluids*. 1992;5:114–122.
31. Catchpole OJ, Grey JB, Noermark KA. Solubility of fish oil components in supercritical co_2 and co_2 + ethanol mixtures *J Chem Eng Data*. 1998;43:1091–1095.

Appendix

The residual Helmholtz energy in the GC-EoS model is described by two terms: a repulsive or free volume term, and a contribution from attractive intermolecular forces

$$\mathrm{A} = \mathrm{A}^{\mathrm{fv}} + \mathrm{A}^{\mathrm{att}} \tag{A1}$$

The free volume contribution is modeled assuming hard sphere behavior for the molecules, characterizing each substance i by a hard-sphere diameter d_i. A Carnahan-Starling type of hard-sphere expression for mixtures is adopted

$$A^{\mathrm{fv}}/RT = 3(\lambda_1\lambda_2/\lambda_3)(\mathrm{Y}-1) + \left(\lambda_2^3/\lambda_3^2\right)(-Y + Y^2 - \ln Y) + n\ln Y \tag{A2}$$

where

$$Y = \left(1 - \frac{\pi\lambda_3}{6\mathrm{V}}\right)^{-1} \quad \text{and} \quad \lambda_k = \sum_i^{NC} n_i d_i^K$$

NC is the number of components, n_i is the number of moles of component i, and V is the total volume. The following temperature-dependent generalized expression is assumed for d_i

$$d_i = 1.065655\, d_{ci}\{1 - 0.12\exp[-2T_{ci}/(3T)]\} \tag{A3}$$

where d_{ci} is the pure component critical hard-sphere diameter, which is calculated as

$$d_{ci} = (0.08943RT_{ci}/P_{ci})^{1/3} \tag{A4}$$

when the compound coincides with a group (e.g., CO_2). Although Eq. A4 can be used to calculate the critical hard-sphere diameter of any molecule, for substances comprising more than a single group, the d_{ci} value is fitted to a point of the pure component vapor pressure curve, usually the normal boiling point. Additionally, vapor pressure data for low volatile or thermolabile substances is often not available or not reliable, and, thus, infinite dilution activity coefficients can be used to estimate the d_{ci} parameter of high-molecular-weight compounds as demonstrated by Espinosa et al.[14]

For the evaluation of the attractive contribution to the Helmholtz energy, a group contribution version of a density-dependent NRTL-type expression is derived

$$A^{\mathrm{att}}/RT = -\frac{z}{2}\sum_i^{NC} n_i \sum_j^{NG} v_j^i q_j \sum_k^{NG} (\theta_k g_{kj}\tilde{q}\rho)/\sum_l^{NG} \theta_l \tau_{lj} \tag{A5}$$

where

$$\theta_j = (q_j/q)\sum_i^{NC} n_i v_j^i \quad q = \sum_i^{NC} n_i \sum_j^{NG} v_j^i q_j$$

$$\tau_{ij} = \exp[\alpha_{ij}\Delta g_{ij}\tilde{q}/(RTV)]$$

$$\Delta g_{ij} = g_{ij} - g_{jj}$$

NG is the number of groups, z is the number of nearest neighbors to any segment (set to 10) v_j^i, the number of groups type j in molecule i, q_j is the number of surface segments assigned to group j, θ_k is the surface fraction of group k, $\tilde{q}$ is the total number of surface segments, g_{ij} is the attraction energy parameter for interactions between groups i and j, and α_{ij} is the NRTL nonrandomness parameter ($\alpha_{ij} \neq \alpha_{ji}$). The interactions between unlike groups are calculated from

$$g_{ij} = K_{ij}(g_{ii}g_{jj})^{1/2} \quad (K_{ij} = K_{ji}) \tag{A6}$$

with the following temperature dependences for the interaction parameters

$$g_{jj} = g_{jj}^*\left(1 + g'_{jj}\left(T/T_j^* - 1\right) + g''_{jj}\ln\left(T/T_j^*\right)\right) \tag{A7}$$

$$K_{ij} = K_{ij}^*\{1 + K'_{ij}\ln[2T/(T_i^* + T_j^*)]\} \tag{A8}$$

where g_{jj}^* is the interaction parameter for reference temperature T_i^*.

Pure group and binary group interaction parameters employed in this work were obtained from Fornari[24] (except for the $K_{TG\text{-}CO2}$ interaction parameter), and are listed in Tables A1 and A2:

Table A1. Pure Group Parameters

	T^*	q	g	g'	g''
CH_3	600.	0.848	316910.	−0.9274	0.0
H_2	600.	0.540	356080.	−0.8755	0.0
CH	600.	0.228	356080.	−0.8755	0.0
CH=CH	600.	0.867	403590.	−0.7631	0.0
AC	600.	0.285	723210.	−0.6060	0.0
ACOH	600.	0.680	1336000.	0.7042	−1.229
ACOC	600.	0.360	514800.	−0.9771	0.0
CH_2COO	600.	1.420	831400.	−1.0930	0.0
$(CH_3COO)_2CH_2COO$ triglyceride group (TG)	600.	3.948	346350.	−1.3460	0.0
CO_2	304.2	1.261	531890.	−0.5780	0.0

Table A2. Binary Group Interaction Parameters

i	j	K_{ij}	K'_{ij}	α_{ij}	α_{ji}
CO_2	CH_3	0.898	0.0	4.683	4.683
	CH_2/CH	0.874	0.0	4.683	4.683
	CH=CH	0.948	0.0	0.0	0.0
	AC	1.074	0.0	−4.772	−4.772
	ACOH	1.094	0.0	0.0	0.0
	ACOC	1.006	0.185	0.0	0.0
	CH_2COO	1.115	0.094	−1.615	−1.615
	TG	1.094	0.112	−1.651	−1.651
	TG[a]	1.190	0.112	−1.651	−1.651
AC	CH_3/CH_2	1.041	0.094	0.391	0.391
	CH	0.980	0.0	0.0	0.0
	ACOH	0.904	0.0	0.0	0.0
	ACOC	0.982	0.0	0.0	0.0
	CH=CH	0.984	0.0	0.0	0.0
	TG	0.986	0.0	0.0	0.0
ACOH	CH_3/CH_2/CH /CH=CH	0.894	0.0	0.0	0.0
	ACOC	1.075	0.0	0.0	0.0
ACOC	CH_3/CH_2/CH/ CH=CH	0.947	0.0	0.0	0.0
TG	CH_3/CH_2/CH	0.860	0.0	0.0	0.0
	CH=CH	0.883	0.0	0.0	0.0
	CH_2COO	1.237	0.0	−8.700	−3.656
CH_2COO	CH_3/CH_2	0.869	0.0	0.0	0.0
	CH=CH	1.006	0.0	−0.876	−0.876

[a]Parameters employed in this work for the TG-CO_2 interaction.

Manuscript received Feb. 19, 2008, and revision received Sept. 1, 2008.